Tensile Deformation of Silver Micro-wires of Small Thickness-to-Grain-Size Ratios

X.X. Chen and A.H.W. Ngan[§]

Department of Mechanical Engineering, The University of Hong Kong,

Pokfulam Road, Hong Kong, P.R. China

[§]Corresponding Author (Email: hwngan@hku.hk; Tel: (852) 25897900; Fax: (852) 25855415)

Abstract

A recent letter from us has indicated that the tensile proof strength of polycrystalline Ag micro-wires, with thicknesses in the range from 20 to 50 μm, depends strongly on the specimen size (t) and weakly on the grain size (d) when t/d becomes smaller than about 3. In this work, we report further coupled effects of specimen size and grain size in the regime when their ratio is small. At a given grain size from 3 to 40 μm, the tensile elongation was found to decrease as the wire thickness decreases, and as the t/d ratio gets smaller than about 3, the tensile elongation loses its dependence on the grain size. The work-hardening rate was found to scale approximately with the proof strength, and so they should be controlled by the same metallurgical factors. Transmission electron microscopy examination of the dislocation microstructures showed that in the regime where the grain size dominates strength and ductility, the dislocation density rises rapidly on deformation, but in the regime where the specimen thickness dominates strength and ductility, the dislocation density remains on the same order of magnitude as the undeformed state. The easy escape of dislocations from the specimen is thought to be the reason for the observed size effect of strength.

Keywords: Yield strength; polycrystalline; tensile elongation; dislocations; size effects; grain size

1. Introduction

The rapid development of design and fabrication of micro-electromechanical systems calls for a need to fully understand the mechanical properties of submicron-to-micron sized materials and structures. One of the most striking phenomena in this regard is that small metal volumes are often stronger than bulk pieces, as reported in early tensile tests on metallic whiskers [1, 2] which revealed extremely high yield strength close to the theoretical limit, as well as a significant size dependence of strength on the whisker thickness. Over the last few decades, tremendous progress has been made towards understanding such a size effect of metal strength, and in the following the different facets of the phenomenon are elucidated in order to indicate what are the unresolved issues, and hence the rationale of this work.

The high strength of metallic whiskers, as mentioned above, was attributed to the absence of pre-existing dislocations in these samples, and so a high stress is needed to nucleate dislocations [1, 2]. On the other hand, a size effect has also been found in situations with high macroscopically imposed plastic strain gradients, as in torsion [3], bending [4] or indentation [5-8]. Thus, traditionally, two important factors enter into the discussion of size effect, namely, whether the sample contains initial dislocations, and whether significant macroscopic plastic strain gradients exist. When the sample contains no initial dislocations, a size effect can be expected based on the premise that a larger sample should contain more sites for dislocation nucleation [9-11], and such a condition is more easily achieved in nanometric sized samples from which any pre-existing dislocations can escape easily [12]. Experiments in such a specimen size regime indeed often revealed size effect [13-17]. The suggestion that plastic strain gradients may play significant roles in plasticity was first coined by Aifantis [18-20]. In the subsequent micro-wire experiments of Fleck et al. [3], since sharp yield points were not observed and the micro-wires used were a dozen to over a hundred microns thick, there is no reason to believe that their samples were initially dislocation free, and indeed no size effect was observed in their tensile experiments. However, they found a significant size effect under torsion, and this led them to propose that the strong plastic strain gradient in torsion was achieved by a high density of geometrically necessary dislocations which then caused extra work hardening. However, unlike Fleck et al.'s tensile results, in recent uniaxial compression tests on sub-micron-to-micron

sized single crystalline pillars, size effect was still observed [12, 14, 21-27] and this is remarkable since compression, like tension, should not be associated with significant macroscopic plastic strain gradients. In these experiments, the micro-pillars also contained initial dislocations, and although they can be squeezed out of the pillar during deformation if the latter's dimension is in the nanometric regime [12], in bigger pillars the dislocation population is never completely depleted during deformation [22], except that it can remain at a low quantity without significant accumulation [25]. It should also be mentioned that the initial dislocations may also be associated with local, microscopic strain gradients [28] and during compression, the deformation is discrete in nature through the occurrence of inhomogeneous slip bands and the end constraints may trigger local crystallographic rotations [29]. However, the roles of such local, microscopic strain gradients on the size effect of strength are far less understood, although a few attempts have been made to model them by the continuum strain-gradient theory [30, 31].

The above amounts to indicate that the absence of pre-existing dislocations, or the presence of strong macroscopic strain gradients, are not the only conditions leading to a size effect of strength. In the case where no initial dislocations exist, the dislocation nucleation process is expected to be size dependent [9-11], but even when dislocations pre-exist, in one theory proposed by Parthasarathy et al. [32], the length of operable sources is expected to scale with the specimen size, leading to a size effect irrespective of whether strong plastic strain gradients exist. In a more recent model [33], the magnitude of the size effect of strength is determined by the sampling with the material volume from an initial dislocation structure of a given spatial distribution of the mesh network. One can then conclude from this body of literature that size effect can arise in different size regimes for different reasons, including dislocation nucleation in initially dislocation-free samples, source activities for samples containing initial dislocations, and work-hardening due to geometrically necessary dislocations for test geometries involving strong strain gradients.

Although the different possible regimes of size effect are elucidated, the above picture still contains one important controversy, namely, Fleck et al.'s tensile tests of micro-wires revealed no size effect [3], but micro-pillar compression experiments, as pioneered by Uchic et al. [21] and used frequently by others as summarized above, consistently revealed significant

size effect of strength. As said above, that the size effect was absent in tension but present in torsion was an important basis for Fleck et al. to suggest that the geometrically necessary dislocations associated with the macroscopically imposed strain gradients cause additional strain-hardening, and this has attracted extensive attention ever since [4, 8 34]. It is important to note that the micro-wires used in Fleck et al.'s experiments were polycrystalline [3] but most micro-pillar compression data reported to-date were single crystalline [12, 14, 21-26]. However, other researchers working on polycrystalline samples also observed significant size effect of strength from tensile tests in the submillimeter regime [35-39]. An important question to ask is therefore: does size effect exist in tension of polycrystalline micro-samples?

To address the above question, we recently carried out tensile tests on silver micro-wires of different thicknesses and grain sizes [40]. The results, reproduced in Figure 1 here for easy reference, indicate that the 0.2% tensile proof stress depends on the wire thickness (t) when the grain size (d) is large, but is insensitive to the specimen thickness when the grain size is small [40]. Figure 1 shows that the Hall-Petch relation was obeyed for the three smallest grain sizes of $< 11\mu m$ studied, irrespective of thickness in the range 20 to $50\mu m$, and in this regime, the specimen thickness did not affect strength. However for the two largest grain sizes 21 and $41\mu m$ studied, the strength was higher than the Hall-Petch trend, and the smaller the thickness, the higher the strength. These results show that there are two distinctive regimes depending on the grain size relative to the specimen size: in the small grain size regime, grain boundary strengthening dominates and strength obeys the Hall-Petch relation while the specimen size is immaterial, and in the large grain size regime, grain boundary strengthening due to the Hall-Petch phenomenon is taken over by a specimen size effect. This finding may explain the above puzzle regarding Fleck et al.'s observation, since it is likely that their grain size relative to the specimen size may fall in the regime where the latter is unimportant in deciding strength.

While the 0.2% proof strength data have been reported in [40], in this paper, we report on other details of the very interesting coupled effects of specimen size and grain size on these micro-wires, including tensile elongation and work-hardening rate. We also report observations from transmission electron microscopy (TEM) examination of the deformation microstructures of the samples.

2. Experimental

The detailed experimental procedures can be found from ref. [40], and here, only the key points are summarized. The coil of silver micro-wire used, of initial thickness ~50 μm, was provided by Dr. George Greene. In the experiments, the wire thickness and grain size were independently varied, by heat treatment the initial wire in a vacuum of 10^{-5} torr for 0.5 hour under different temperatures from 170 to 750°C to vary the grain size, followed by etching in 65% nitric acid for different times to obtain different wire thicknesses for each grain size. The resultant grain sizes and wire thicknesses were in the ranges of 3 to 41 μm, and 20 to 50 μm, respectively. The polycrystalline microstructure and further details of the tested wires can be seen from Figure 1 and Table 1 of ref. [40]. It is also worthy to note that the etching procedure used did not result in extensive pitting on the wires' surface, as can be seen by comparing the scanning electron microscopy (SEM) images of the as-received (~50 μm) and an etched (~40 μm) wire in Figure 2.

Tensile tests were performed in an Agilent Technology T150 UTM tensile tester, the construction of which is illustrated in Figure 3(a). To perform the test, the wire sample was glued by epoxy resin onto a paper template with a diamond shaped window cut out in the middle, as shown in Figure 3(b). The template-specimen assembly was then mounted onto the two grips of the tensile machine, and then the two sides of the paper template were carefully cut open to free out the wire sample. The height of the diamond shaped window of the paper template was 20mm, which was taken as the gauge length of the sample. The tests were conducted at a nominal strain rate of $5\times10^{-4}\,s^{-1}$ at room temperature. In some of the tests the wire broke at or near the epoxy resin glue, and the corresponding data were excluded from the subsequent analysis. To check for repeatability and/or scatter of the results, the test was repeated for each condition, until the number of valid data was typically 6 to 11. After the tensile tests, TEM examination of the deformation microstructures was carried out. Longitudinal sections along the wire axis were exposed by focused-ion beam (FIB) milling in a FEI Quanta 200 3D Dual Beam FIB/SEM system, as shown in the example in Figure 4(a). TEM foils inclined at ~45º to the

tensile axis were fabricated by milled out ditches on such exposed longitudinal surfaces as shown in Figure 4(b).

3. Results

3.1 Flow instabilities

Recent tensile experiments on micron-sized specimens [17, 24] were carried out using a nanoindenter travelling in the reverse, tensile direction, with a specially made diamond nanoindenter tip hooking onto the T-shaped head of the specimen which was in the form of a micro-pillar attached to a firm base. In such a test mode, the transducer has the nanometric displacement resolution required for the purpose, and since the micro-pillar specimen is usually only a few to tens of microns long, the tensile elongations encountered can be provided simply by the motion of the movable core of the transducer, the allowable range of which is typically a few microns. Such a test mode, however, is not applicable for testing wires with gauge lengths in the millimeter range, since the tensile elongation encountered would far exceed the allowable movement of the transducer. For this reason, a special tensile tester supplied by Agilent Technology Inc. was used in this work. This tester has a transducer similar to that of an Agilent's nanoindenter, and so the nominal displacement resolution is also in the nanometric regime which is sufficient. However, as shown in Figure 3(a), the other end of the wire specimen is not fixed to a firm base as in the above-mentioned test mode [17, 24], but is made to travel upward at a constant speed so as to elongate the specimen on the way. The movable part of the transducer, onto which the lower end of the wire specimen is attached as shown in Figure 3(a), is a spring-suspended pull rod which connects to the electromagnetic coil of a linear motor. The linear motor exerts a downward force, which is measured from the electromagnetic coil's current, to counteract the upward pulling force on the specimen by the upper grip. The movement of the lower pull rod relative to the machine's frame is measured by a capacitive gage, and feedback control is applied to the linear motor so as to maintain the lower pull rod, and hence the lower end of the wire specimen, at an approximately constant height level. This construction allows large tensile elongations in the sample to happen while the capacitive gage only needs to detect

error displacement signals, which could be submicron, for the feedback control. This is a rather unique setup available commercially at present for nanomechanical work in the tensile mode, but as at today, its use has not been widely reported in the literature.

As discussed above and as illustrated in Figure 3(a), although the transducer itself has nanometric resolution, the wire specimen is effectively floating in space during the test, since both of its ends are attached to movable parts of the machine. The achievable resolution of the elongation of the specimen, therefore, is determined not solely by the transducer's own resolution but also by the sensitivity of the feedback mechanism which serves to keep the lower end of the specimen at a constant height level. The ability to do so is clearly pivotal to the interpretation of the test data, but this is an aspect which has never been discussed before in the open literature. For this reason, before reliable tests could be conducted on the wire samples, we investigated the effect of the proportional–integral–derivative (PID) control parameters on the test result. We first discovered that if the gain of the PID control is set to a high value, a slight softening event in the wire specimen will cause the linear motor at the bottom to over-react by excessively unloading the specimen, and this would have the effect of very sensitively detecting small instability events during deformation [41]. Figure 5 shows such an example from an as-received ~50 μm diameter Ag micro-wire. With the control parameters concerned, ripples were seen in the engineering stress (σ) – engineering strain (ε) curve in Figure 5(a), and these grew bigger towards the later stage of the deformation near fracture. After the strain level of ~0.1, each of the big oscillations consisted of unload, often into the elastic range, followed by reload. Corresponding to these ripples were large oscillations of the center-plate in the capacitive gage, as shown in Figure 5(b), which indicate the over-reaction of the control loop at the set parameters. If the deformation of the sample were smooth, the center plate would have no reason to suddenly jump, and so the ripple events must be caused by sudden softening of the sample. Thus, at some point during deformation, the Ag sample softened and elongated suddenly, causing the center plate to suddenly drop. The feedback loop reduced the current in the linear motor to decrease load, but this was over-done, and so the specimen might even be unloaded into the elastic regime. Then the control reacted to load up again, forming one ripple. The same set of control parameters as in Figure 5 was used to test a batch of 80 μm polypropylene wires (results not shown), and no obvious oscillations were found in the stress-strain curves, and the center

plate oscillations were less than $\pm 2\mu m$, which is much smaller than those in the Ag microwire case ($\pm$ 60 to 80 μm). This serves to indicate that the big ripples observed in the Ag micro-wires were triggered by sudden softening events, or "strain bursts" as these are called in the literature.

With the control parameters set according to those in Figure 5, strain burst events, which are commonly found during plastic deformation of crystals [21-23, 42], were usually seen in the Ag wires tested. While these sudden events can be made more conspicuous this way, the excessive unloading and reloading may cause repercussions to the microstructure and the subsequent deformation, and so the subsequent events may be triggered to occur in a somewhat artificial way. For this reason, in all subsequent tests, the PID feedback control parameters were changed from PID = (0.01, 0.0002, 0.001) to (0.5, 0.00001, 0.005), at which the center plate position could be made more stable during the deformation. At such conditions, the ripples in the stress-strain response were no longer observable, and Figure 6 shows one example. Here, the average amplitude of the center plate position oscillation was around ±2μm, which is similar to the magnitude encountered in the control experiments with the polypropylene wires. With a gage length of 20mm, such movements of the center-plate mean that the strain during the tests was controlled to an accuracy of around 0.01%. All test data reported in the following, and in ref. [40], were obtained using the same PID control parameters as in Figure 6.

3.2 Strength and Ductility

Representative stress-strain curves can be found from ref. [40], and Figure 1 summarises the 0.2% proof strengths. Figure 7 shows the work-hardening rate $d\sigma/d\epsilon$ measured at 0.2% strain vs the proof stress at the same strain, at different wire thickness and gain size. It can be seen that the data fall in a narrow band corresponding to a proportionality relation between the two parameters, i.e. the mechanisms controlling yield strength and work-hardening seem to be the same. The % elongation of the wires with different thicknesses and grain sizes is shown in Figure 8. The data there indicate that for a given specimen thickness, elongation decreases as grain size increases, and for a given grain size elongation decreases as the specimen becomes thinner. However, when the wire thickness to grain size ratio is lower than about 3, the dependence on grain size weakens, and elongation is dominated by the wire thickness. This

corresponds well to the 0.2% proof stress data shown in Figure 1, where strength depends less on grain size but depends more strongly on specimen size in the same regime of *t*/*d* less than about 3. Figure 9 shows the typical appearances of fractured 40μm thick Ag wires with different grain sizes. For the samples with small grain sizes of 3.5 and 5.1 μm shown in Figure 9(a) and (b) respectively, ductile fracture with extensive necking can be seen, but for the larger grain sizes of 21.0 and 40.6 μm shown in Figure 9(c) and (d) respectively, knife-edge like brittle rupture occurred with traces of slip bands and deformation twinning seen.

3.3 Dislocation density measurements

As shown in Figure 4(b), TEM samples at ~45° from the tensile axis were cut from the fracturing ends of the deformed samples to investigate the dislocation structure and density. Figure 10 shows the bright-field TEM images of an undeformed 750°C-annealed Ag wire with the largest grain size of 40μm. Figure 10(a-c) were taken near the [112] pole at $g = (2\bar{2}0)$, $(1\bar{1}\bar{1})$ and $(2\bar{2}0)$ respectively, and (d) was taken near the [101] pole at $g = (\bar{1}11)$. From these images, the undeformed wire of d ~ 40μm contained pre-existing dislocations of density ~$1.5\times10^{14}\ m^{-2}$. Figures 11(a-d) show the TEM images taken with different diffraction vectors of an undeformed 170°C-annealed Ag wire, and Figure 12 is a lower magnification montage showing the polycrystalline structure with grain size ~5μm. Again, dislocations pre-existed in such an undeformed sample, with density ~$2.2\times10^{14}\,m^{-2}$. The contrast of the dislocations in these images was higher and wider than usual, and this is likely to be due to the segregation of gallium atoms to the dislocation cores during the FIB milling process. In Figures 11(d) and 12(b), the distinguished condition of $\boldsymbol{g}\cdot\boldsymbol{b}=0$ was met, but still significant residual contrast remained due possibly to the decoration by gallium atoms.

Figure 13(a-d) show the TEM images of a deformed 750°C-annealed Ag wire with grain size ~40μm and thickness ~50μm, to an elongation of 0.12, and Figure 14 shows a low-magnification montage the same sample. The dislocation density in this sample near the fracture point is ~$2.8\times10^{14}\ m^{-2}$, i.e. it underwent a mild increase by ~87% comparing with the initial dislocation density of ~$1.5\times10^{14}\ m^{-2}$. Figure 15 shows a TEM montage near the fracture point of

a deformed 170°C-annealed wire of thickness ~ 40 μm and initial grain size ~ 5μm, with elongation 0.14. Despite the elongation in this case is only marginally higher than that in Figures 13 and 14, the dislocation density of this wire is $\sim 1\times 10^{16}\ m^{-2}$, about two orders of magnitude higher than that of the undeformed wire, as well as the deformed sample in Figures 13 and 14. Details of the TEM samples and their corresponding figures are given in Table 1.

In addition to the dislocation densities, the dislocation structures inside the different Ag wires also differ. The undeformed wires in Figures 10 to 12 exhibited organized dislocation structures similar to those observed in other annealed metals. In the deformed samples, some clustering of dislocations can be seen in Figure 14, and cell structures can be seen in Figure 15.

4. Discussion

One important finding in the present study is the existence of two separate regimes in which the grain size or the specimen size determines strength. From the 0.2% proof stress data in Figure 1, the transition grain size is about 10μm, and since the thickness varies from ~20 to 50 μm, the transition t/d ratio is about 2 to 5, i.e. a few. When the t/d ratio is above this transition value, the Hall-Petch effect prevails and grain size determines strength, and when t/d is below the transition, specimen thickness t has a strong effect on strength. Interestingly, the tensile elongation in Figure 8 also exhibits a transition across the t/d ratio of about 2 to 5: for larger t/d ratios tensile elongation is large and increases as the grain size reduces, and for lower t/d ratios the tensile elongation is lower and is independent of the grain size, but increases as the thickness t increases. A transition in deformation mechanism is therefore pertinent across the t/d ratio of about 2 to 5.

The TEM dislocation structures shown in Figures 10 to 15 belong to two groups above and below the transition at $t/d \sim 2$ to 5. As summarized in Table 1, the 750°C-annealed wires with thickness 50μm have $t/d = 1.2$ which falls in the domain where strength and elongation are affected by specimen size but not grain size, and the 170°C-annealed wires with thickness 40μm have $t/d = 7.8$ which falls in the domain where grain size significantly affects strength and elongation. Yet, these two groups of samples had similar elongation of 0.12 and 0.14

respectively, and similar initial dislocation density on the order of 10^{14} m^{-2}. Interestingly, the smaller grained wire had the dislocation density increased by nearly two orders of magnitude to 10^{16} m^{-2} after tensile elongation, but the larger grained wire had the dislocation density remaining at the same order of magnitude 10^{14} m^{-2} after elongation. This remarkable difference in the extent of dislocation production and accumulation is likely to be the reason for why in one case the grain size controls strength and elongation and in the other case it is specimen thickness that has a major role. In the high t/d ratio regime, many grain boundaries are present and they trap dislocations inside the grains and act as sources to produce new ones, and hence the generation and storage of dislocations are high. The grain size in this case therefore significantly affects strength and fracture, and this regime may be referred to as the intrinsic size effect which is simply the Hall-Petch effect. In the low t/d ratio regime, only a few or sometimes no grain boundaries are present across the specimen thickness, and so dislocations once generated can slip out of the specimen, so that accumulation is low. The scarcity of grain boundaries also limits the sourcing of dislocations, and so dislocation production is also low. In this case, the specimen thickness has a strong influence on the escape of generated dislocations as well as the sourcing of new dislocations, and this is probably why strength and elongation strongly depend on specimen size in this regime. This regime may be referred to as the extrinsic size effect since it is the specimen's dimension, not its microstructure, which plays a major role.

In the regime where specimen size affects strength, more careful analysis of the strength data suggests the existence of a shape effect which depends on the value of the t/d ratio, and an absolute size effect which depends on t only, and the interested reader is referred to our recent publication [40]. In terms of the shape effect which depends on t/d, it should be noted that macro-plasticity theory actually predicts that when t/d is small, the strength should be *lower*, not higher, than the case when t/d is large [37]. This is because when there are only a few grains across the specimen thickness, the volume fraction of grains which are exposed to free surfaces is high, but these grains are subjected to less constraints and are thus easier to deform. Janssen et al. [36] and Keller et al. [39] observed such a "smaller being weaker" effect in tensile tests on specimens of sizes in the sub-millimeter range, i.e. in hundreds of microns. The present observation of a "smaller being stronger" effect is pertinent to specimen thicknesses in the micron regime, and is therefore more akin to the size effect observed from the recent micro-pillar

compression experiments. Although dislocation dynamics have been used to successfully predict the size effect of strength in single crystals [32, 43-45] dislocation dynamics simulations on polycrystals with limited specimen size have so far been limited, but in the few studies performed so far, no specimen size dependence of strength could be captured in addition to the Hall-Petch effect [46, 47], or no clear trend can be observed [48]. It should also be mentioned that in this regime where there are only a few grains across the specimen's thickness, the parameter t/d may not be the sole indicator of the size effect – apart from the average dimensions t and d, the grain boundary arrangement may also be a critical factor. In any case, the regime where t/d is small deserves more thorough investigation in the future.

5. Conclusions

The present experiments reveal the existence of a regime where the specimen size dominates over grain size in affecting the tensile strength, work-hardening rate and elongation. This happens for micron-sized specimens when the ratio of specimen thickness to grain size is smaller than a critical value of ~ 2 to 5, and the smaller the specimen size, the higher the strength and the lower the elongation. TEM examination of the dislocation microstructure suggests that the low ability for dislocations to accumulate inside the specimen is likely the reason for the existence of this regime.

Acknowledgments

We thank Dr. George Greene for providing the Ag wire. The work described in this paper was supported by a grant from the Research Grants Council of the Hong Kong Special Administration Region, P.R. China (Project No. HKU7159/10E).

References

[1] Brenner S. S., 1956. Tensile strength of whiskers. Journal of Applied Physics. 27, 1484-1491.

[2] Brenner S. S., 1957. Plastic deformation of copper and silver whiskers. Journal of Applied Physics. 28, 1023-1026.

[3] Fleck N. A., Muller G. M., Ashby M. F., Hutchinson J. W., 1994. Strain gradient plasticity: thoery and experiment. Acta Metallurgica et Materialia. 42, 475-487.

[4] Stolken J. S., Evans A. G., 1998. A microbend test method for measuring the plasticity length scale. Acta Materialia. 46, 5109-5115.

[5] Doerner M. F., Nix W. D., 1986. A method for interpreting the data from depth-sensing indentation instruments. Journal of Materials Research. 1, 601-609.

[6] Ma Q. Clarke D. R., 1995. Size dependent hardness of silver single crystals. Journal of Materials Research. 10, 853-863.

[7] McElhaney K. W., Vlassak J. J., Nix W. D., 1998. Determination of indenter tip geometry and indentation contact area for depth-sensing indentation experiments. Journal of Materials Research. 13, 1300-1306.

[8] Nix W. D., Gao H., 1998. Indentation size effects in crystalline materials: a law for strain gradient plasticity. Journal of the Mechanics and Physics of Solids. 46, 411-425.

[9] Zuo L., Ngan A. H. W., Zheng G. P., 2005. Size dependence of incipient dislocation plasticity in Ni_3Al. Physical Review Letters. 94, 095501-095504.

[10] Ngan A. H. W., Zuo L., Wo P. C., 2006. Probabilistic nature of the nucleation of dislocations in an applied stress field. Scripta Materialia. 54, 589-593.

[11] Zuo L., Ngan A. H. W., 2006. Molecular dynamics study on compressive yield strength in Ni3Al micro-pillars. Philosophical magazine letters. 86, 355-36.

[12] Shan Z. W., Mishra R., Asif S. A. S., Warren O. L., Minor A. M., 2007. Mechanical annealing and source-limited deformation in submicrometre-diameter Ni crystals. Nature Materials. 7, 115-119.

[13] Wu B., Heidelberg A. Boland J. J., 2005. Mechanical properties of ultrahigh-strength gold nanowires. Nature Materials. 4, 525-529.

[14] Kim J. Y., Greer J. R., 2009. Tensile and compressive behavior of gold and molybdenum single crystals at the nano-scale. Acta Materialia. 57, 5245-5253.

[15] Jennings A. T., Burek M. J., Greer J. R., 2010. Microstructure versus size: mechanical properties of electroplated singlecrystalline Cu nanopillars. Physical Review Letters. 104, 135503-135506.

[16] Jennings A. T., Greer J. R., 2011. Tensile deformation of electroplated copper nanopillars. Philosophical Magazine. 91, 1108-1120.

[17] Kim J.Y., Jang D., Greer J.R., 2011. Crystallographic orientation and size dependence of tension-compression asymmetry in molybdenum nano-pillars, International Journal of Plasticity, in press.

[18] Aifantis, E.C., 1984. On the microstructural origin of certain inelastic models. Journal of Engineering Materials and Technology. 106, 326–330.

[19] Aifantis, E. C., 1999. Strain gradient interpretation of size effects. International Journal of Fracture. 95, 229-314.

[20] Aifantis, E.C., 2003. Update on a class of gradient theories. Mechanics of Materials. 35 259–280.

[21] Uchic M. D., Dimiduk D. M., Florando J. N., Nix W. D., 2004. Sample dimensions influence strength and crystal plasticity. Science. 305, 986-989.

[22] Dimiduk D. M., Uchic M. D. Parthasarathy T. A., 2005. Size-affected single-slip behavior of pure nickel microcrystals. Acta Materialia. 53, 4065-4077.

[23] Greer J. R., Oliver W. C., Nix W. D., 2005. Size dependence of mechanical properties of gold at the micron scale in the absence of strain gradients. Acta Materialia. 53, 1821-1830.

[24] Kiener D., Grosinger W., Dehm G., Pippan R., 2008. A further step towards an understanding of size-dependent crystal plasticity: in situ tension experiments of miniaturized single-crystal copper samples. Acta Materialia. 56, 580-592.

[25] Ng K. S., Ngan A. H. W., 2008. Stochastic nature of plasticity of aluminum micro-pillars. Acta Materialia. 56, 1712-1720.

[26] Richter G., Hillerich K., Gianola D. S., Monig R., Kraft O., Volkert C.A., 2009. Ultrahigh strength single crystalline nanowhiskers grown by physical vapor deposition. Nano Letters. 9, 3048-3052.

[27] Kaufmann D., Mönig, R., Volkert C. A., Kraft O., 2011. Size dependent mechanical behaviour of tantalum. International Journal of Plasticity. 27, 470-478.

[28] Maaß R., Van Petegem S., Borca C.N., Van Swygenhoven H., 2009. Probing strains and dislocation gradients with diffraction. Materials Science and Engineering A, 524, 40-45.

[29] Maaß R., Van Petegem S., Grolimund D., Van Swygenhoven H., Kiener D., Dehm G., 2008. Crystal rotation in Cu single crystal micropillars: *In situ* Laue and electron backscatter diffraction. Applied Physics Letters. 92, 071905-1-3.

[30] Tsagrakis I., Konstantinidis A., Aifantis E.C., 2003. Size effects in tension: gradient internal variable and wavelet models. Journal for the Mechanical Behaviour of Materials. 14, 41-58.

[31] Zhang X., Aifantis K.E., 2011. Interpreting strain bursts and size effects in micropillars using gradient plasticity. Materials Science and Engineering A. 528, 5036-5053.

[32] Parthasarathy T. A., Rao S. I., Dimiduk D. M., Uchic M. D., Trinkleb D. R., 2007. Contribution to size effect of yield strength from the stochastics of dislocation source lengths in finite samples. Scripta Materialia. 56, 313-316.

[33] Ngan A.H.W., 2011. An explanation for the power-law scaling of size effect of strength in micro-specimens. Scripta Materialia. 65, 978-981.

[34] Swadener J. G., George E. P., Pharr G. M., 2002. The correlation of the indentation size effect measured with indenters of various shapes. Journal of the Mechanics and Physics of Solids. 50, 681-694.

[35] Simons G., Weippert Ch., Dual J., Vllain J., 2006. Size effects in tensile testing of thin cold rolled and annealed Cu foils. Materials Science and Engineering A. 416, 290-299.

[36] Janssen P. J. M., Keijser Th. H. de, Geers M. G. D., 2006. An experimental assessment of grain size effects in the uniaxial straining of thin Al sheet with a few grains across the thickness. Materials Science and Engineering A. 419, 238-248.

[37] Geers M. G. D., Brekelmans W. A. M., Janssen P. J. M., 2006. Size effects in miniaturized polycrystalline FCC samples: strengthening versus weakening. International Journal of Solids and Structures. 43, 7304-7321.

[38] Lederer M., Groger V., Khatibi G., Weiss B., 2010. Size dependency of mechanical properties of high purity aluminium foils. Materials Science and Engineering A. 527, 590-599.

[39] Keller C., Hug E., Feaugas X., 2011. Microstructural size effects on mechanical properties of high purity nickel. International Journal of Plasticity. 27, 635-654.

[40] Chen X. X., Ngan A. H. W., 2011. Specimen size and grain size effects on tensile strength of Ag microwires. Scripta Materialia. 64, 717-720.

[41] Miguel M. C, Zapperi S., 2006. Fluctuations in plasticity at the microscale. Science. 312, 1151-1152.

[42] Volkert C. A., Lilleodden E.T., 2006. Size effects in the deformation of sub-micron Au columns. Philosophical Magazine. 86, 5567-5579.

[43] El-Awady J. A., Wen M., Ghoniem N. M., 2009. The role of the weakest-link mechanism in controlling the plasticity of micropillars. Journal of the Mechanics and Physics of Solids. 57, 32-50.

[44] Akarapu S., Zbib H. M., Bahr D. F., 2010. Analysis of heterogeneous deformation and dislocation dynamics in single crystal micropillars under compression. International Journal of Plasticity. 26, 239-257.

[45] El-Awady J. A., Rao S. I., Woodward C., Dimiduk D. M., Uchic M. D., 2011. Trapping and escape of dislocations in micro-crystals with external and internal barriers. International Journal of Plasticity. 27, 372-387.

[46] Balint D. S., Deshpande V. S., Needleman A., Van der Giessen E., 2006. Size effects in uniaxial deformation of single and polycrystals: a discrete dislocation plasticity analysis. Modelling and Simulations in Materials Science and Engineering. 14, 409-422.

[47] Li Z., Hou C., Huang M., Ouyang C., 2009. Strengthening mechanism in micro-polycrystals with penetrable grain boundaries by discrete dislocation dynamics simulation and Hall-Petch effect. Computational Materials Science. 46, 1124-1134.

[48] Fan H., Li Z., Huang M., Zhang X., 2011. Thickness effects in polycrystalline thin films: surface constraint versus interior constraint. International Journal of Solids and Structures. 48, 1754-1766.

Table 1. Dislocation densities of the undeformed and deformed Ag wires

	Annealing temperature (°C)	Grain size *d* (μm)	Wire thickness *t* (μm)	*t*/*d* ratio	Elongation (mm/mm)	Dislocation density * (m^{-2})	Figure
Undeformed	750	40.6	50	1.2	0	1.5×10^{14}	10
	170	5.1	40	7.8	0	2.2×10^{14}	11, 12
Deformed	750	40.6	50	1.2	0.12	2.8×10^{14}	13, 14
	170	5.1	40	7.8	0.14	1×10^{16}	15

* Here, the dislocation density is estimated as 1/(dislocation spacing)^2.

Figures

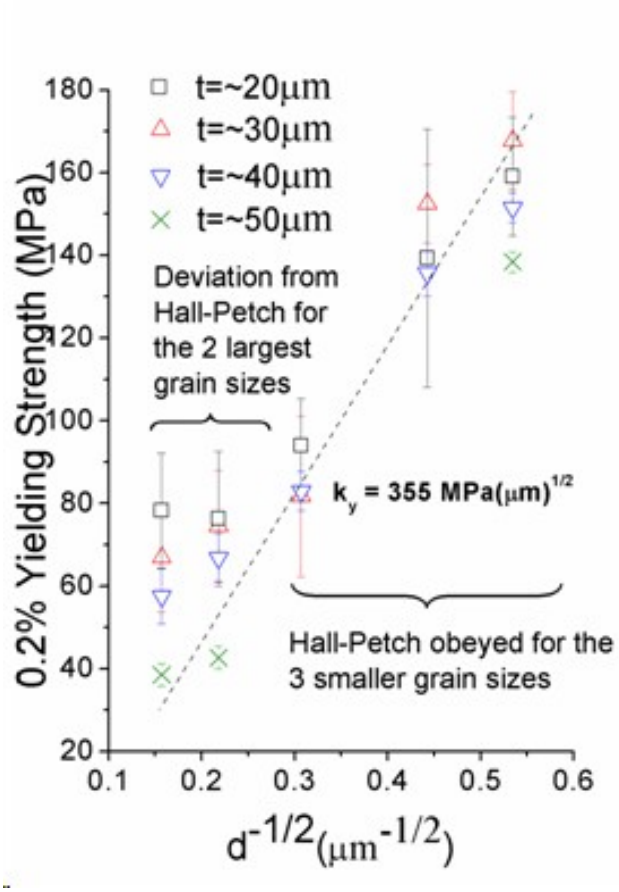

Figure 1. Hall-Petch relationship applied to the 0.2% yielding strength (specimen thickness: 50, 40, 30 and 20 μm). Error bars denote ±1 standard deviation. Reproduced from ref. [40].

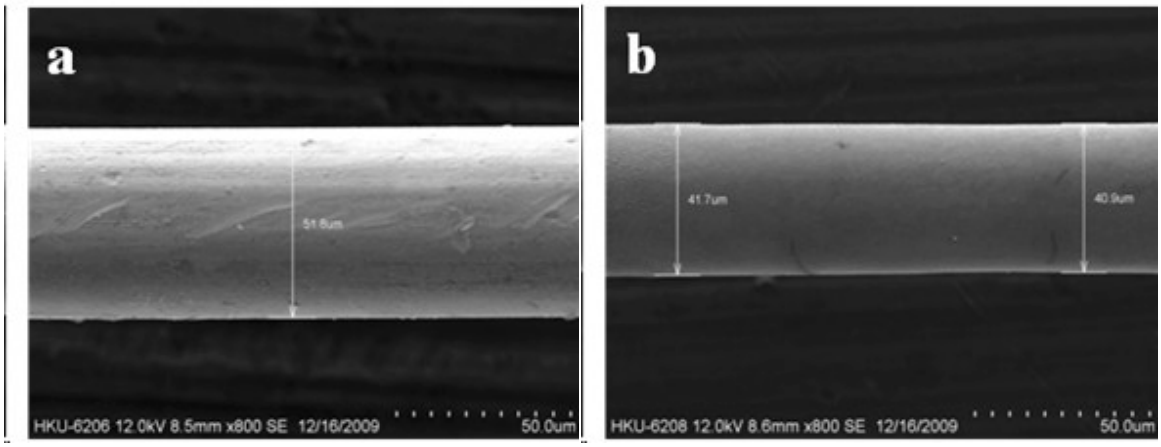

Figure 2. SEM images of the (a) as-received (~50 μm) and (b) etched (~40 μm) wires.

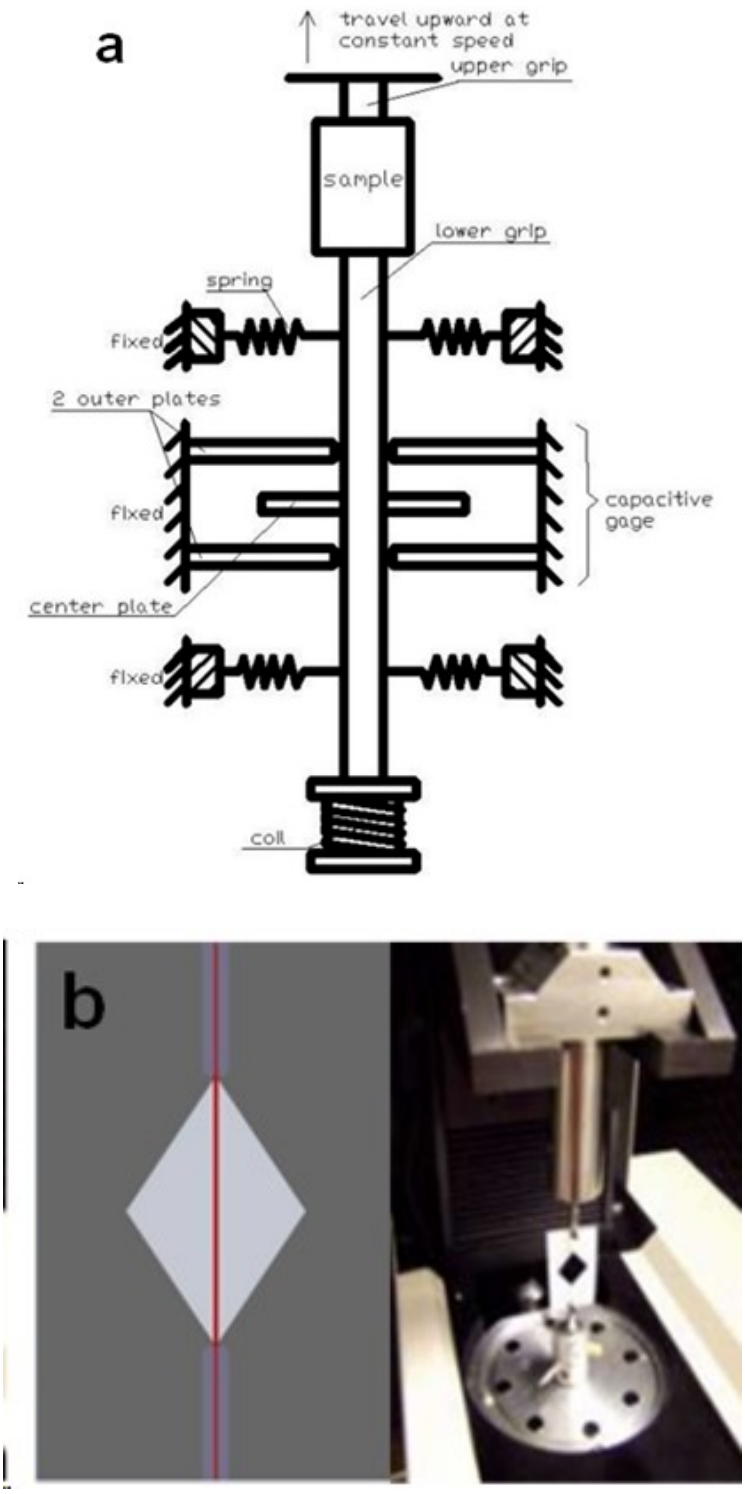

Figure 3. (a) Schematic of the Nano UTM system, (b) schematic of the paper template with the wire specimen, and photograph of an actual specimen mounted on the tensile machine.

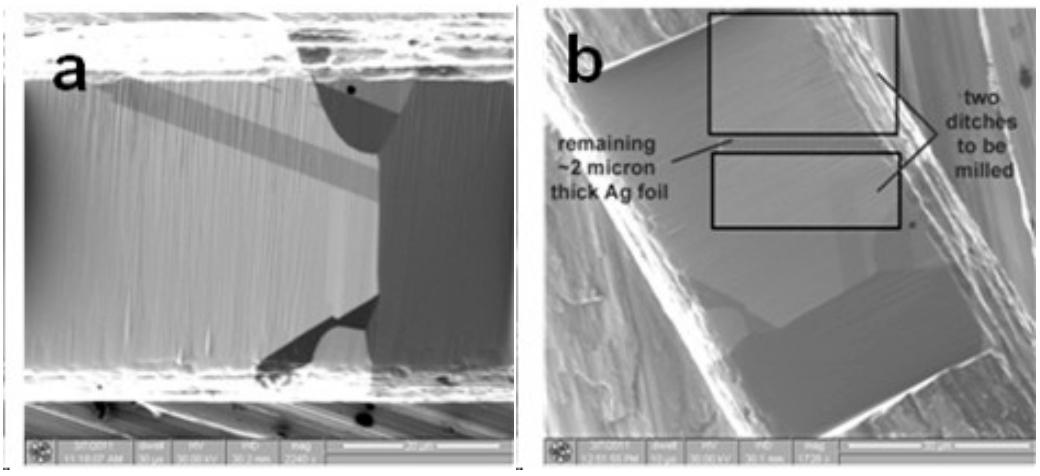

Figure 4. FIB milling for SEM/TEM observation. (a) A surface portion of the wire is milled away to expose a longitudinal section of the specimen. (b) Two ditches to be milled on the exposed longitudinal section to leave behind a TEM foil which is inclined at ~45º to the tensile axis. The foil is subsequently freed away by milling along its periphery, and transferred to a TEM sample grid by the Omniprobe.

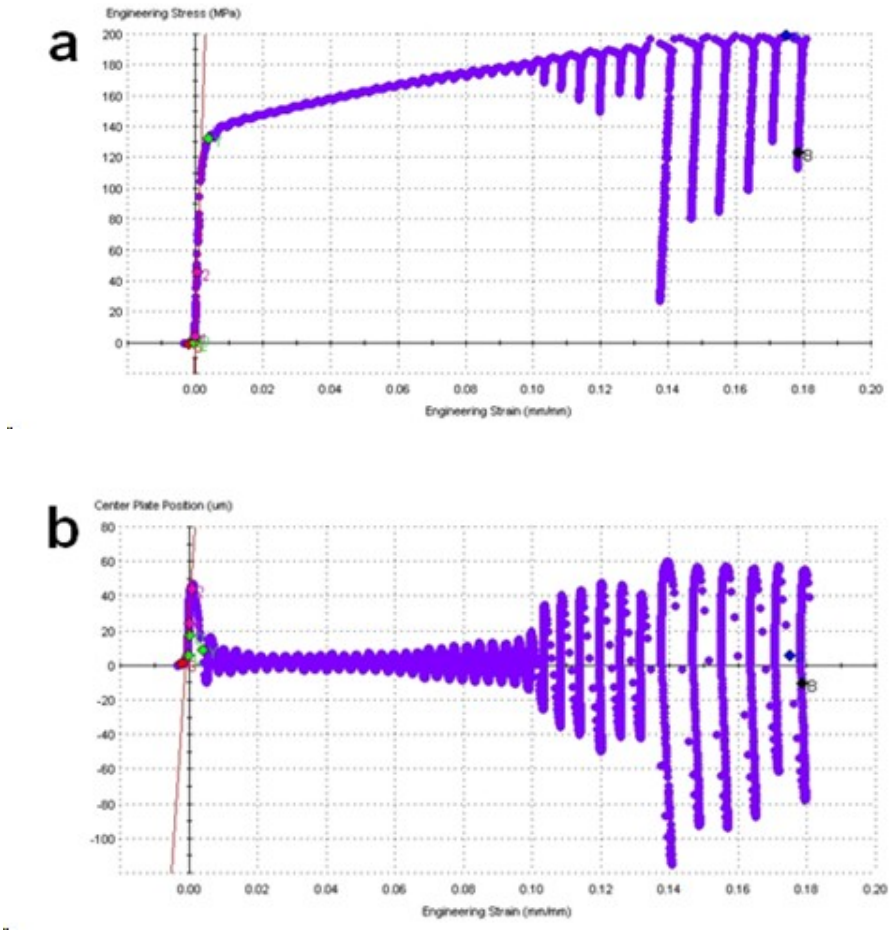

Figure 5. (a) Typical engineering stress - engineering strain curve with big ripples obtained with PID control parameter changes of PID = (0.01, 0.0002, 0.001), and (b) its correspongding center plateposition - engineering strain curve.

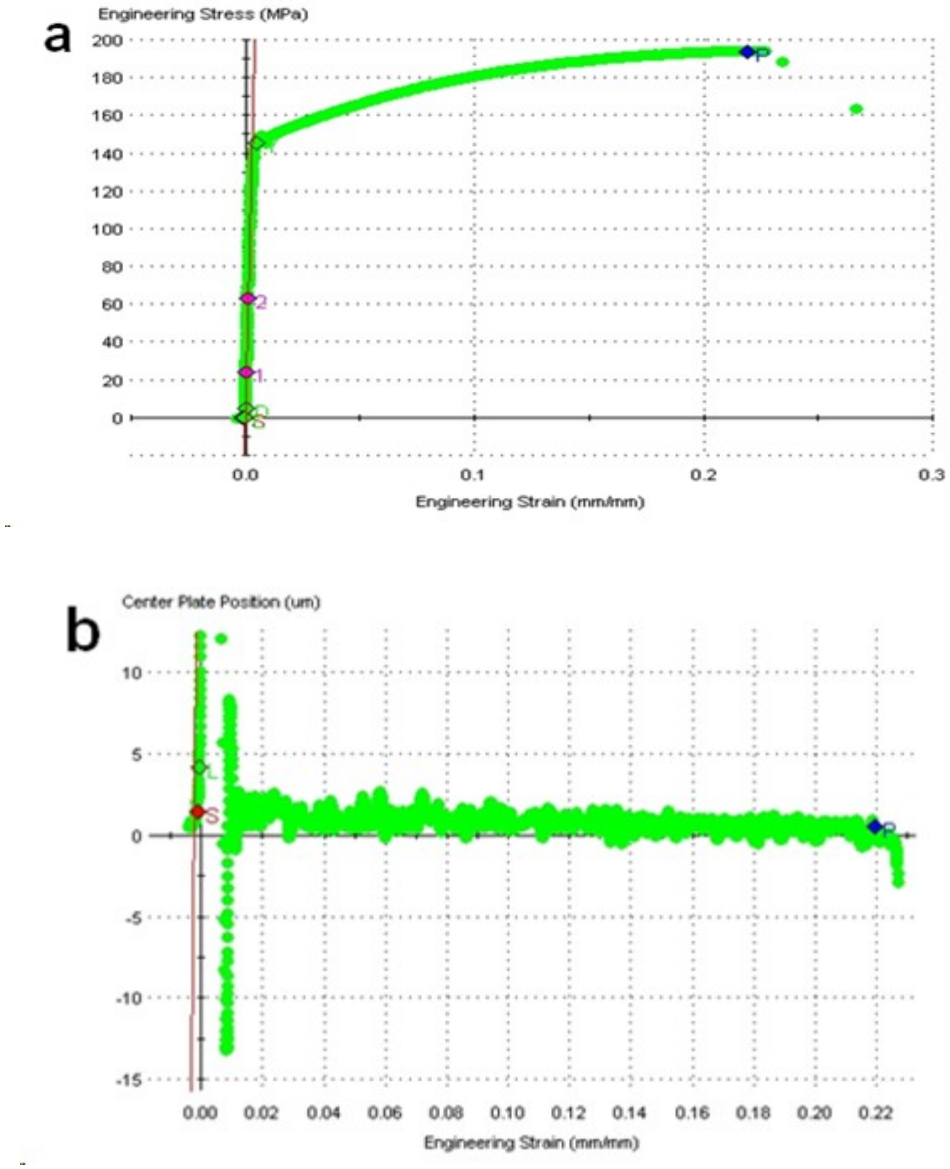

Figure 6. (a) Typical engineering stress - engineering strain curve at the later set of control parameters of PID = (0.5, 0.00001, 0.005), and (b) its correspongding center plateposition - engineering strain curve.

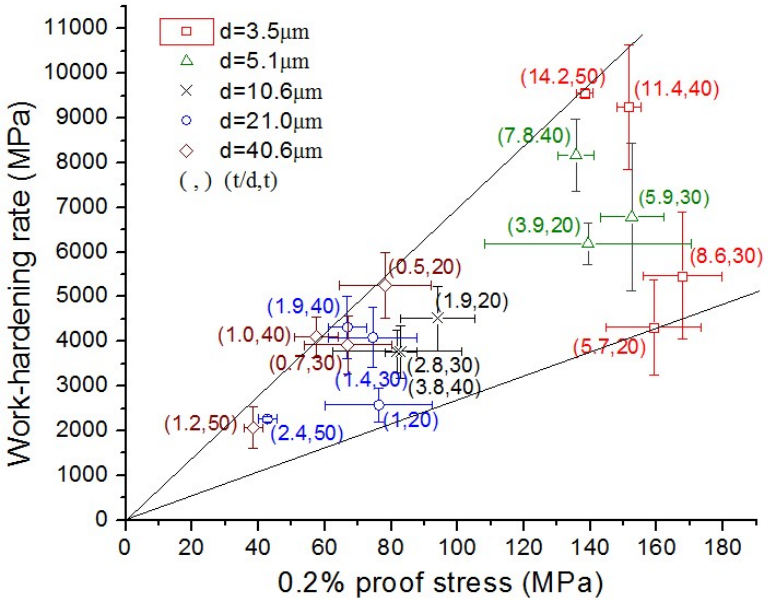

Figure 7. Working-hardening rate at 0.2% vs the proof stress at the same strain, at different specimen thickness and grain size.

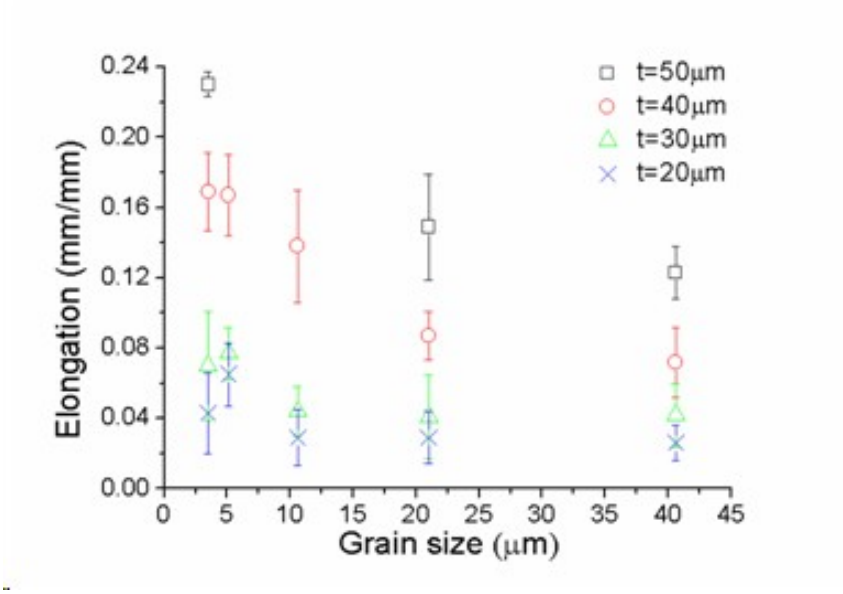

Figure 8. Elongation – grain size graphs of Ag wires with different wire thicknesses (*t*). Error bars denote ±1 standard deviation. (a) *t*=20 μm, (b) *t*=30 μm, (c) *t*=40 μm, (d) *t*=50 μm.

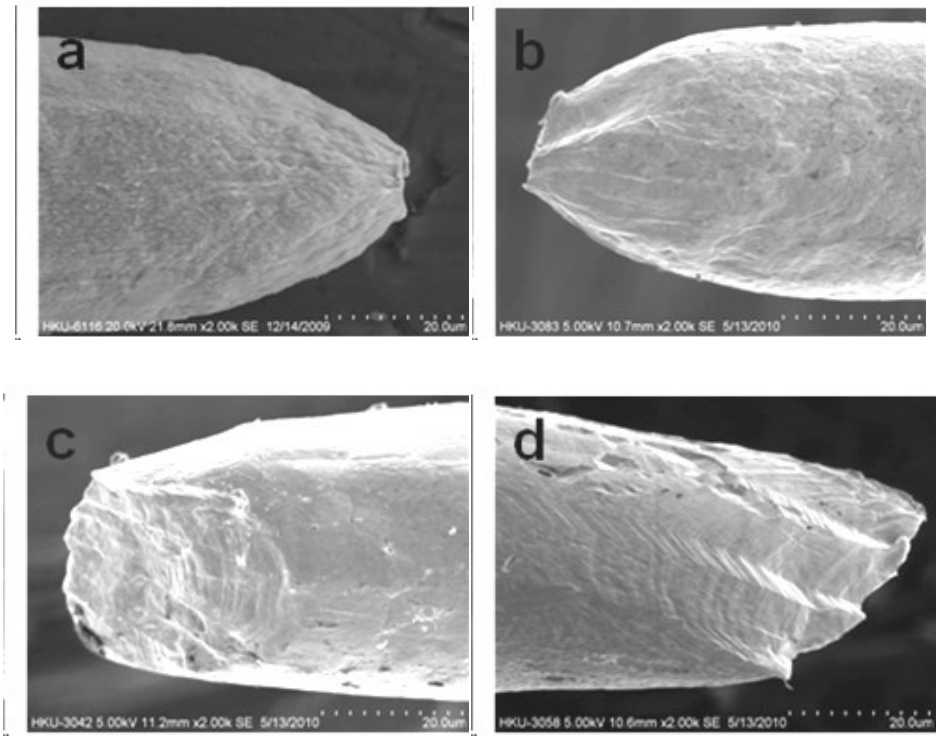

Figure 9. SEM fractographs of 40μm thick-Ag wires after deformation. Grain size *d* = (a) 3.5 μm, (b) 5.1 μm, (c) 21.0 μm, (d) 40.6 μm.

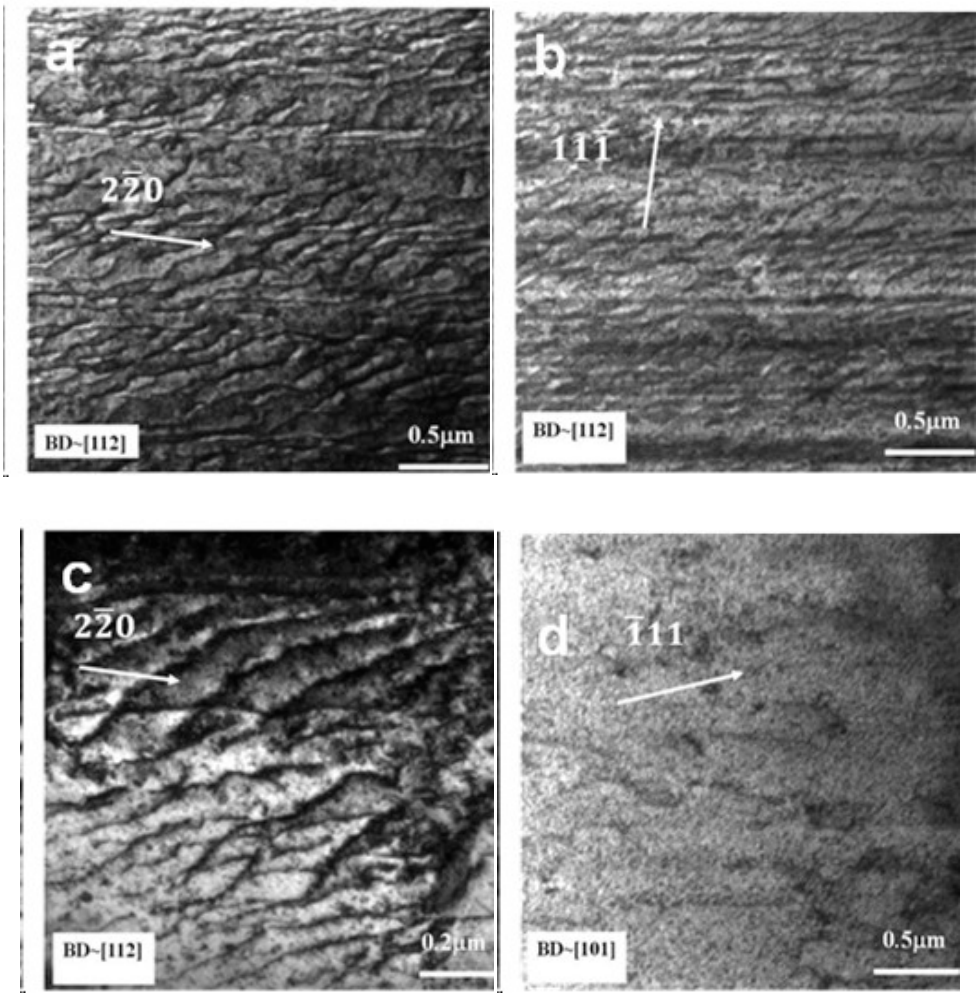

Figure 10. TEM dislocation structures in undeformed, 750°C-annealed Ag wire with grain size of 40μm.

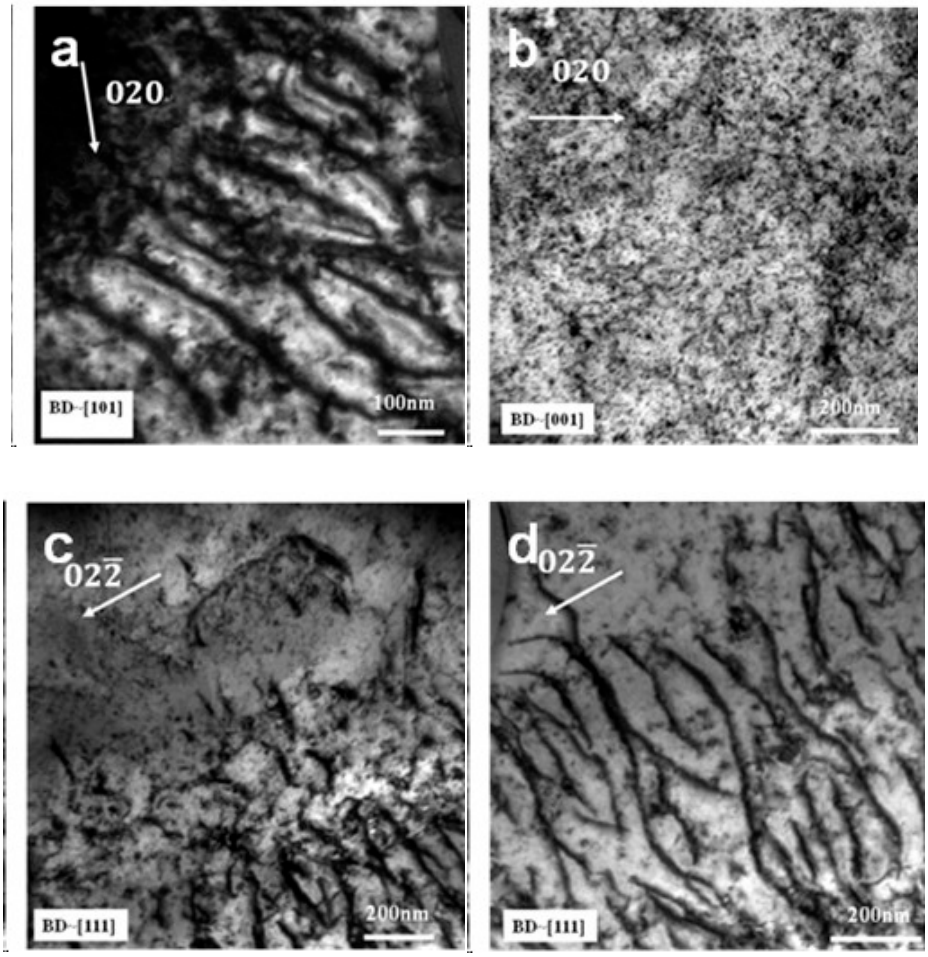

Figure 11. TEM images of the undeformed 170°-annealed Ag wire with grain size ~ 5μm.

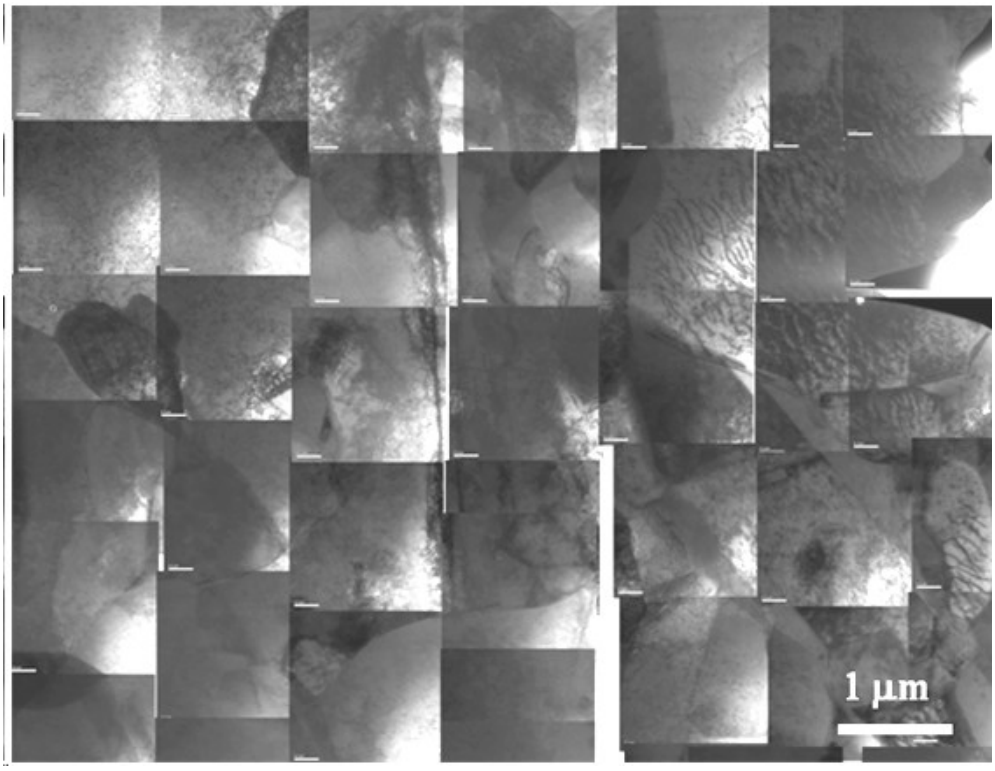

Figure 12. A lower magnification montage of TEM images of the undeformed 170°C–annealed Ag wire showing the polycrystalline structure with grain size ~ 5µm and the pre-existing dislocations inside the grains.

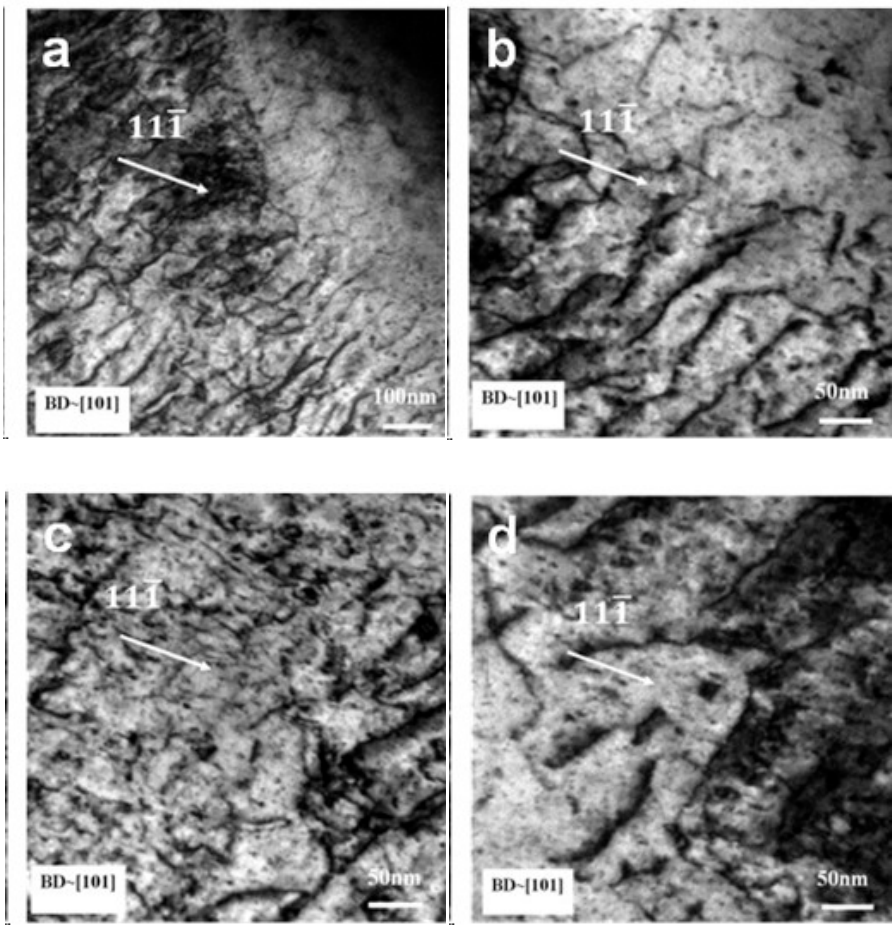

Figure 13. TEM images of a deformed 750°C-annealed Ag wire of thickness ~50μm and grain size ~40μm, near the fracture point.

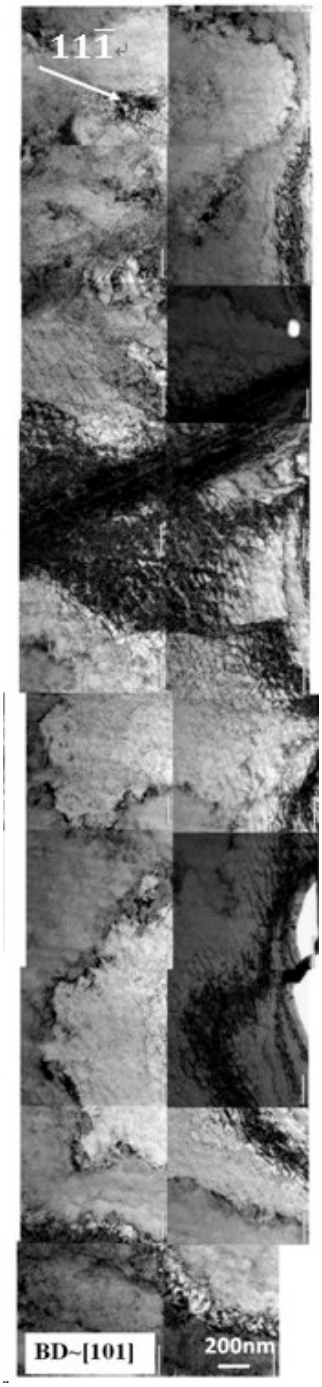

Figure 14. A montage of TEM images of the same sample as Figure 13.

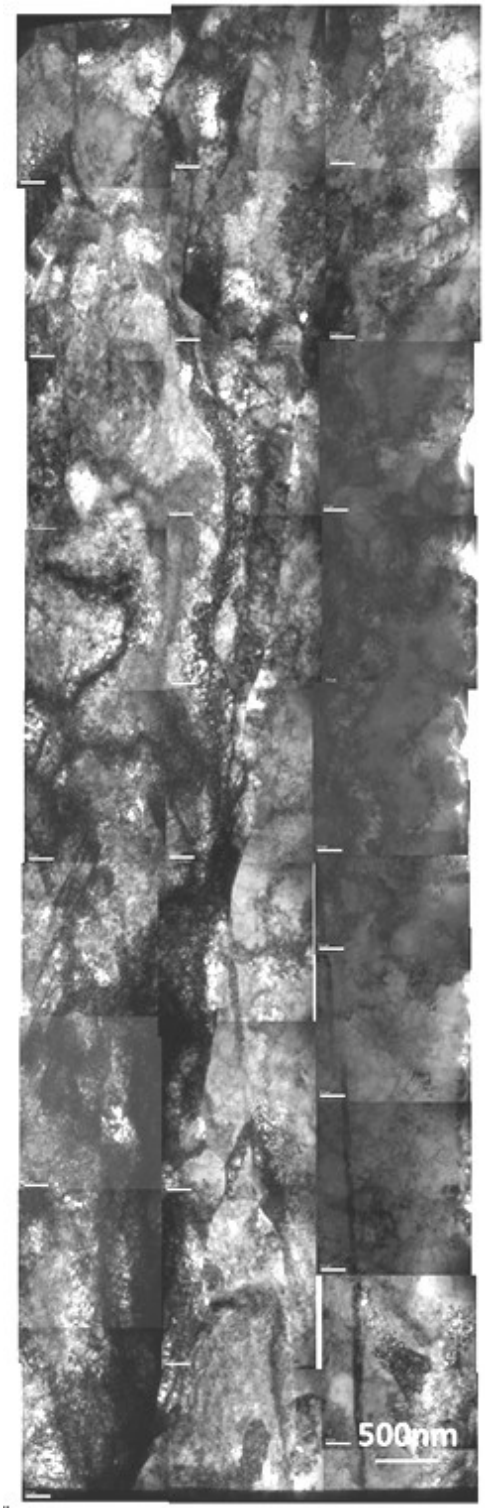

Figure 15. A montage of TEM images of the deformed 170°C-annealed Ag wire of thickness ~40 μm and initial grain size ~5μm near the fracture point.